

Simultaneous Electrochemical Generation of Ferrate and Oxygen Radicals to Blue BR Dye Degradation

Authors:

Mauricio Chilibingua, Patricio J. Espinoza-Montero, Oscar Rodríguez, Alain Picos, Erick R. Bandala, S. Gutiérrez-Granados, Juan M. Peralta-Hernández

Date Submitted: 2020-10-06

Keywords: BBR dye, ferrate ion, electro-oxidation, advance oxidation processes (AOP)

Abstract:

In this study, electro-oxidation (EOx) and in situ generation of ferrate ions [Fe(VI)] were tested to treat water contaminated with Blue BR dye (BBR) using a boron-doped diamond (BDD) anode. Two electrolytic media (0.1 M HClO₄ and 0.05 M Na₂SO₄) were evaluated for the BDD, which simultaneously produced oxygen radicals (•OH) and [Fe(VI)]. The generation of [Fe(VI)] was characterized by cyclic voltammetry (CV) and the effect of different current intensity values (e.g., 7 mA cm⁻², 15 mA cm⁻², and 30 mA cm⁻²) was assessed during BBR degradation tests. The discoloration of BBR was followed by UV-Vis spectrophotometry. When the EOx process was used alone, only 78% BBR discoloration was achieved. The best electrochemical discoloration conditions were found using 0.05 M Na₂SO₄ and 30 mA cm⁻². Using these conditions, overall BBR discoloration values up to 98%, 95%, and 87% with 12 mM, 6 mM, and 1 mM of FeSO₄, respectively, were achieved. In the case of chemical oxygen demand (COD) reduction, the EOx process showed only a 37% COD reduction, whereas combining [Fe(VI)] generation using 12 mM of FeSO₄ achieved an up to 61% COD reduction after 90 min. The evolution of reaction byproducts (oxalic acid) was performed using liquid chromatography analysis.

Record Type: Published Article

Submitted To: LAPSE (Living Archive for Process Systems Engineering)

Citation (overall record, always the latest version):

LAPSE:2020.1020

Citation (this specific file, latest version):

LAPSE:2020.1020-1

Citation (this specific file, this version):




LAPSE:2020.1020-1v1

DOI of Published Version: <https://doi.org/10.3390/pr8070753>

License: Creative Commons Attribution 4.0 International (CC BY 4.0)

Article

Simultaneous Electrochemical Generation of Ferrate and Oxygen Radicals to Blue BR Dye Degradation

Mauricio Chilingua ^{1,2}, Patricio J. Espinoza-Montero ^{3,*} , Oscar Rodríguez ², Alain Picos ², Erick R. Bandala ⁴ , S. Gutiérrez-Granados ² and Juan M. Peralta-Hernández ^{2,*} 

¹ Departamento de Ingeniería Civil y Ambiental, Facultad de Ingeniería Civil y Ambiental, Escuela Politécnica Nacional. P.O. Box, Quito 17-01-2759, Ecuador; mauricioacade14@hotmail.com

² Departamento de Química, División de Ciencias Naturales y Exactas, Universidad de Guanajuato, Cerro de la Venada s/n, Pueblito de Rocha, Guanajuato 36040, Mexico; om.rodrigueznarvaez@ugto.mx (O.R.); picosbrother@hotmail.com (A.P.); gutigs59@hotmail.com (S.G.-G.)

³ Escuela de Ciencias Químicas, Pontificia Universidad Católica del Ecuador, Avenida 12 de Octubre y Roca, Apartado, Quito 17-01-2184, Ecuador

⁴ Division of Hydrologic Sciences, Desert Research Institute, 755 E. Flamingo Road, Las Vegas, NV 89119-7363, USA; Erick.Bandala@dri.edu

* Correspondence: pespinoza646@puce.edu.ec (P.J.E.-M.); juan.peralta@ugto.mx (J.M.P.-H.); Tel.: +593-2299-1700 (ext. 1929) (P.J.E.-M.); +52-4737327555 (ext. 5416) (J.M.P.-H.)

Received: 10 March 2020; Accepted: 25 June 2020; Published: 28 June 2020



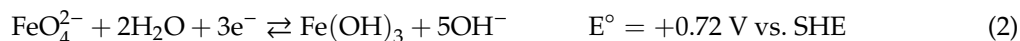
Abstract: In this study, electro-oxidation (EOx) and in situ generation of ferrate ions [Fe(VI)] were tested to treat water contaminated with Blue BR dye (BBR) using a boron-doped diamond (BDD) anode. Two electrolytic media (0.1 M HClO₄ and 0.05 M Na₂SO₄) were evaluated for the BDD, which simultaneously produced oxygen radicals (\bullet OH) and [Fe(VI)]. The generation of [Fe(VI)] was characterized by cyclic voltammetry (CV) and the effect of different current intensity values (e.g., 7 mA cm⁻², 15 mA cm⁻², and 30 mA cm⁻²) was assessed during BBR degradation tests. The discoloration of BBR was followed by UV-Vis spectrophotometry. When the EOx process was used alone, only 78% BBR discoloration was achieved. The best electrochemical discoloration conditions were found using 0.05 M Na₂SO₄ and 30 mA cm⁻². Using these conditions, overall BBR discoloration values up to 98%, 95%, and 87% with 12 mM, 6 mM, and 1 mM of FeSO₄, respectively, were achieved. In the case of chemical oxygen demand (COD) reduction, the EOx process showed only a 37% COD reduction, whereas combining [Fe(VI)] generation using 12 mM of FeSO₄ achieved an up to 61% COD reduction after 90 min. The evolution of reaction byproducts (oxalic acid) was performed using liquid chromatography analysis.

Keywords: advance oxidation processes (AOP); electro-oxidation; ferrate ion; BBR dye

1. Introduction

Industrial effluents contain a wide variety of pollutants that are potentially harmful to humans, such as dyes and organic compounds, and most of these pollutants are difficult to remove using conventional water treatment systems (e.g., physicochemical, and/or biological processes) [1]. When released into the environment without the proper treatment, these effluents produce significant fluctuations in water quality parameters such as chemical oxygen demand (COD), biological oxygen demand (BOD), pH, color, and/or salinity [2], which increase public concerns when the proper treatments are not being implemented. Therefore, finding alternative treatment processes that are suitable to remove highly recalcitrant pollutants in industrial wastewater effluents is a pending science and technology need.

An alternative for water treatment known since the 1970s has been ferrate(VI) ion (FeO_4^{2-}), a very strong, chemically green oxidizer, highly stable in aqueous medium, especially at alkaline and neutral pH, where iron shows oxidation state +6 [3–6]. However, we must emphasize that ferrate's highest oxidizing power occurs preferably in an acidic medium, and decreases in alkaline pH (reaction 1 and 2) [4,7].



Ferrate anions can exist in various oxidation states: $[\text{FeO}_4]^{2-}$ with Fe(VI), $[\text{FeO}_4]^{3-}$ with Fe(V) or $[\text{FeO}_4]^{4-}$ with Fe(IV) [8]. However, Fe(VI) is the most stable form with broad industrial uses. The unique chemical properties of ferrate (VI) include:

- High redox potential, with the ability to oxidize harmful organic and inorganic species such as nitrosamines, phenol, nitrilotriacetic acid, hydrazine, thiourea, sulfides, cyanide, thioacetamide, ammonia, thiocyanate, soluble oils, as well as inactivate viruses and bacteria [5,8–11].
- A bifunctional ability to act as oxidizing and coagulating agent, due to the simultaneous release of ferric ions (Fe(III)), specifically under neutral or alkaline conditions [12–14].
- A higher redox potential than other oxidizers commonly used for water treatment such as chlorine (1.358 V vs. SHE), hydrogen peroxide (1.776 V vs. SHE), and ozone (2.076 V vs. SHE) [15].
- Ferrate use prevents the formation of carcinogenic disinfection byproducts (mainly trihalomethanes).
- It generates non-toxic reduction byproducts such as Fe(III) and Fe(II), which can be used for other purposes.
- Ferrate can also be used for biofouling control and for the removal of other contaminants such as metals, non-metals, and radionuclides [16–18].

Boron-doped diamond (BDD) electrodes have an inert surface, a wide electrochemical window, low adsorption, high corrosion resistance, and electrochemical stability. These electrodes are also considered a suitable surface upon which to carry out electro-oxidation (EOx) processes [19]. They have greater O_2 evolution overpotential than other electrodes (e.g., Pt and PbO_2) and low water oxidation reaction, combined with the capability to generate large amounts of oxygen radicals (e.g., $\bullet\text{OH}$) [20]. Recent studies suggest that ferrate ions can be generated in situ from Fe(II) salts using a BDD anode surface under acidic conditions (0.1 M HClO_4) by applying a potential of 2.2 V vs. NHE [21].

Despite the existing information about the potential of ferrate for water treatment [22–27] and the attractive features of its generation in situ by EOx processes, more research is needed to identify the best reaction conditions to treat complex industrial effluents using this technology. The goal of this work was to investigate the best conditions to generate ferrate ions in situ using a BDD electrode by cyclic voltammetry as well as assess the feasibility of using in situ generated ferrate simultaneously with the EOx process to degrade a textile dye (e.g., Blue BR (BBR) dye), following water discoloration, COD abatement, as well as an assessment of the evolution of reaction byproducts (e.g., carboxylic acids).

As is well known, the interest in studying the electrochemical generation of the ferrate ion on boron-doped diamond (BDD) electrodes, has gained great relevance; this due to its potential applications in the environmental area, specifically in water treatment. This paper presents results on the simultaneous production of the ferrate ion and free radicals on a BDD surface; studies of the generation of both species in two different electrolytes and with the addition of different concentrations of iron sulfate are presented, we also study the effect of the current density on the degradation of an industrial dye; for this, the level of discoloration, reduction in COD and the evolution of a byproduct, namely carboxylic acid, are considered. We consider this research to be relevant because we present important results on how the action of both oxidants generated on the same electrode simultaneously will improve the degradation of the dye, which enhances its application in water treatment.

2. Materials and Methods

2.1. Materials

All reagents used in this investigation—perchloric acid (HClO_4), ferrous sulfate ($\text{FeSO}_4 \cdot 7\text{H}_2\text{O}$), sodium sulfate (Na_2SO_4), and sulfuric acid (H_2SO_4)—were obtained from Aldrich and J.T. Baker and used without any purification. The industrial grade BBR dye ($\text{C}_{32}\text{H}_{28}\text{N}_2\text{Na}_2\text{O}_8\text{S}_2$), widely used in the tanning industry in Mexico, was supplied by PCL (Guanajuato, Mexico). The BDD electrode was obtained from MetakemTM (Germany).

2.2. Electrochemical Characterization

The redox behavior of FeSO_4 on BDD was evaluated by CV, employing a three-electrode cell: BDD as an anode (0.5 cm^2), Pt wire as a counter electrode, and Ag/AgCl as the reference electrode, using the BASi potentiostat/galvanostat and Epsilon-EC software at a scan rate ranging from 100 mV s^{-1} to 500 mV s^{-1} . As an electrolyte (blank), we used 0.1 M HClO_4 with 6 mM of FeSO_4 as analyte.

Additionally, the electrochemical response by cyclic voltammetry (CV) of three FeSO_4 concentrations (1 mM , 6 mM , and 12 mM), in two different electrolytes 0.1 M HClO_4 and $0.05 \text{ M Na}_2\text{SO}_4$ (adjusted to pH 3 with H_2SO_4) was evaluated. The experiments were performed in a three-electrode electrochemical cell (25 mL), using a BDD (0.5 cm^2) plate as a working electrode, platinum (Pt) wire as a counter electrode, and Ag/AgCl as a reference electrode. The CV tests were performed using a BASi Epsilon potentiostat/galvanostat. Specific concentrations of FeSO_4 were prepared from a stock solution in 100 mL of distilled water and added to the media in all the [Fe(VI)] production experiments.

2.3. Electrochemical Set Up

The discoloration assays were carried out in galvanostatic mode using three different current density values (e.g., 7 mA cm^2 , 15 mA cm^2 , and 30 mA cm^2) in a 100 mL tank reactor with constant magnetic stirring (200 rpm). One initial BBR dye concentration (50 mg/L) was used for all the experimental trials. The BBR dye (chemical formula = $\text{C}_{32}\text{H}_{28}\text{N}_2\text{Na}_2\text{O}_8\text{S}_2$, molecular weight = 678.68 g/mol , and $\lambda_{\text{max}} = 695 \text{ nm}$) was used in this study. An accurately weighed quantity of the dye was dissolved in distilled water to prepare the stock solution (100 mg L^{-1}). Experimental solutions of desired concentration (50 mg/L) were obtained by successive dilution. The surface area of the BDD anode was 2.5 cm^2 and a Pt wire was used as the cathode. The study solution was monitored for color reduction using a UV-Vis spectrophotometer (Cintra 1010 device) at $\lambda = 695 \text{ nm}$ [27].

Water discoloration was carried out by testing two electrolytic media: 0.1 M HClO_4 and $0.05 \text{ M Na}_2\text{SO}_4$ adjusted to pH 3 with H_2SO_4 . In both cases, three different FeSO_4 concentrations (1 mM , 6 mM , and 12 mM) were tested. To evaluate the amount of remaining oxidable material in solution, the chemical oxygen demand (COD) was quantified according to the Standard Methods (method 5220D); total nitrogen concentration was also estimated by the Standard Methods [28].

For the different parameters tested, the kinetics approach of the combined electrochemical degradation of BBR dye was determined by a pseudo-first order model, $\ln(A_0/A_t) = kt$, where A_0 is the initial absorbance, A_t is the absorbance after degradation time t , and k is the apparent rate constant.

Carboxylic acids were identified and quantified by ion-exclusion HPLC using an Agilent Technologies 1260 Infinity Series with a Bio-Rad Aminex HPX 87H ($300 \text{ mm} \times 7.8 \text{ mm}$) column at $35 \text{ }^\circ\text{C}$ and by setting the photodiode detector at $\lambda = 210 \text{ nm}$. For these determinations, $20 \text{ } \mu\text{L}$ of the sample was injected into the HPLC, using 4 mM of H_2SO_4 as the mobile phase and flow rate 0.8 mL/min [29–32]. The quantification of the COD was carried out only for the best BBR degradation conditions (e.g., electrolytic solution of 0.05 M of Na_2SO_4 at a pH of 3, current density of 30 mA cm^{-2} , and 12 mM of FeSO_4) following the Standard Methods [29].

3. Results and Discussion

3.1. Cyclic Voltammetric (CV) Study

Figure 1 shows the redox behavior of 6 mM of FeSO_4 on BDD at different scan rates (100 mV s^{-1} to 500 mV s^{-1}) using 0.1 M HClO_4 as electrolyte. It is worth emphasizing that the linear behavior of the second peaks agree with the Randles–Sevcik equation (I_p vs. $(\text{scan rate})^{1/2}$) (data not shown), indicating a diffusion-controlled process where the redox species are not adsorbed on the surface of the electrode [33]. In this study, oxidation peaks from Fe(II) to Fe(III) were observed at 0.54 V vs. Ag/AgCl, the overoxidation of Fe(III) to $[\text{Fe(VI)}]$ was found at 0.90 V vs. Ag/AgCl, and reduction to Fe(II) was identified at 0.25 V vs. Ag/AgCl. These results support the theory of in situ formation of $[\text{Fe(VI)}]$ on the BDD surface, as shown in Figure 1 [34]. In Figure 2 the electrogeneration of the ferrate ion can be confirmed as the concentration of FeSO_4 increases both the oxidation signal from Fe(II) to Fe(III) and the oxidation signal from Fe(III) to $[\text{Fe(VI)}]$ increases proportionally. The number of oxidation and reduction signals matches with those described for Figure 1, even though a slight displacement in the potential axis was observed, probably related to the amount of FeSO_4 used for the media. However, ferrate ion production was found to increase as the concentration of FeSO_4 increased [35]. In a previous work, our research group suggested ferrate ion formation at potential values close to 2.5 V Ag/AgCl, using 0.1 M HClO_4 [21,35]. The difference in the oxidation and over-oxidation reaction behavior of Fe(II) to Fe(III) and Fe(VI), respectively, observed in this study could be related to the composition of the electrode surface (C-sp²/C-sp³ ratio), usage time, and the composition of BDD during its syntheses (e.g., doping level, or precursor used) [36].

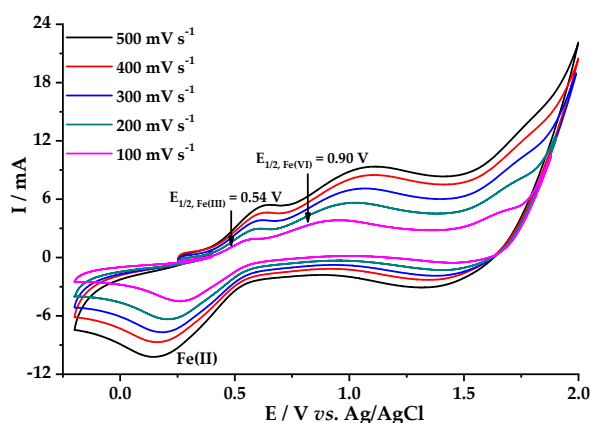


Figure 1. Behavior of 6 mM FeSO_4 at different voltammetric scan rate, in 0.1 M HClO_4 , on $0.5 \text{ boron-doped diamond (BDD) cm}^2$ as working electrode; counter electrode—platinum wire.

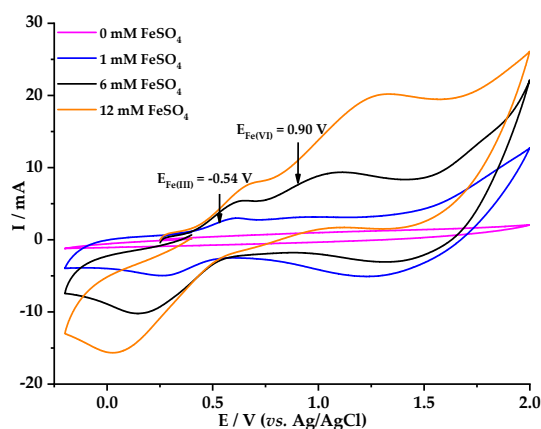


Figure 2. Voltammetric response of FeSO_4 at different concentrations in 0.1 M HClO_4 , with BDD 0.5 cm^2 as working electrode, scanning speed 50 mV s^{-1} ; counter electrode—platinum wire.

Figure 3 shows the redox behavior of 6 mM FeSO₄ on BDD, at different scan rates (50 mV s⁻¹ to 100 mV s⁻¹) using 0.05 M Na₂SO₄ as electrolyte after adjusting pH to 3 with concentrated H₂SO₄. Two signals for oxidation from Fe(II) to Fe(III) at -0.30 V vs. Ag/AgCl were identified, plus another for overoxidation of Fe(II) to Fe(VI) at 0.78 V vs. Ag/AgCl. Figure 4 shows the effect of FeSO₄ concentration when a constant scan rate (50 mV s⁻¹) was used. It is worth noting that at increased concentrations of FeSO₄, the oxidation and reduction signals increase slightly and move significantly towards higher values of both oxidation and reduction potential. In addition, the second oxidation signal appeared at a lower potential value when Na₂SO₄ was used as the electrolyte (0.78 V, Figure 4), compared with the signal obtained when HClO₄ was used as the electrolyte (0.90 V, Figure 2). Therefore, better degradation of BBR would be expected when Na₂SO₄ is used as the electrolyte, as this reaction media would favor the formation of ferrate ion at lower potential values [37].

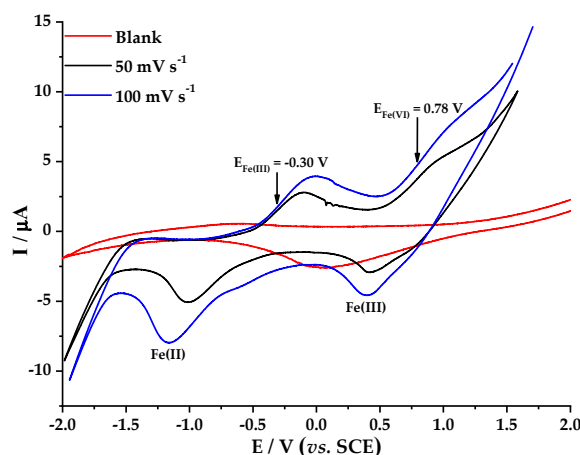


Figure 3. Behavior of 6 mM FeSO₄ at different voltammetric scan rate, 0.05 M Na₂SO₄, on BDD 0.5 cm² as working electrode; counter electrode—platinum wire.

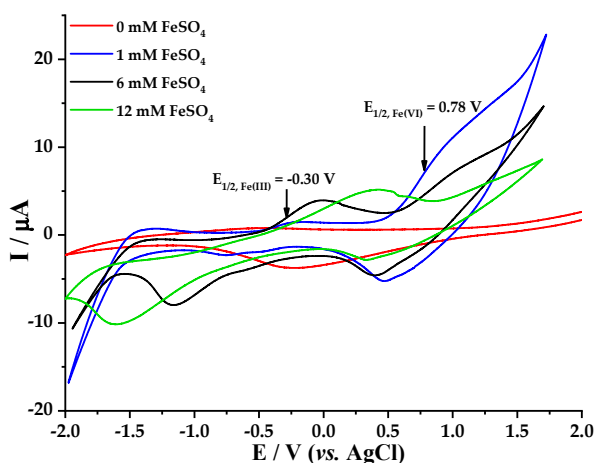


Figure 4. Voltammetric response of FeSO₄ at different concentrations, 0.05 M Na₂SO₄, on BDD 0.5 cm² as working electrode, scan rate 50 mV s⁻¹; counter electrode—platinum wire.

3.2. BBR Dye Degradation

3.2.1. Effect of the Electrolyte on the EOX Discoloration Process

The effect of the electrolyte type on the EOX discoloration was explored first. Figure 5 shows the discoloration curves as a function of reaction time for HClO₄ (Figure 5a) and Na₂SO₄ (Figure 5b) at the different current density values tested (e.g., 7 mA cm⁻², 15 mA cm⁻², and 30 mA cm⁻²). As shown, no significant difference was found when the lower current density (7 mA cm⁻²) was tested

independently of the electrolyte type used. Nevertheless, a significant difference was found when higher current density values were tested. For example, an overall discoloration of 23% was achieved using 15 mA cm^{-2} and 0.1 M HClO_4 , whereas up to 62% of overall discoloration (over twice the amount achieved reached for HClO_4) was achieved when $0.05 \text{ M Na}_2\text{SO}_4$ was used as the electrolyte.

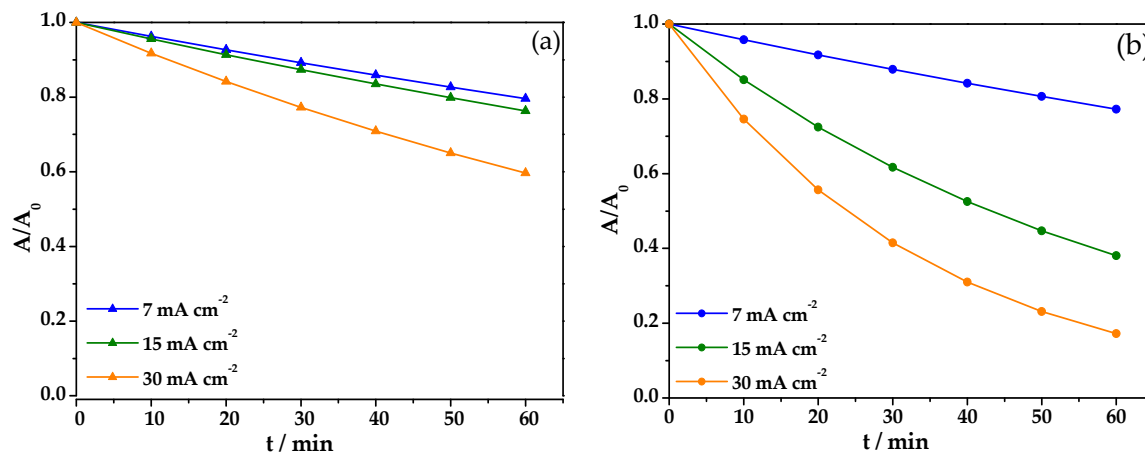


Figure 5. Removal of an aqueous solution of Blue BR (BBR) azo dye, $C_0 = 50 \text{ mg/L}$, during the oxidation process in (a) 0.1 M HClO_4 and (b) $0.05 \text{ M Na}_2\text{SO}_4$ with a solution volume of 0.1 L .

When the highest current density (30 mA cm^{-2}) was tested, the overall water discoloration achieved after 60 min was 49% for 0.1 M HClO_4 , whereas the trials using $0.05 \text{ M Na}_2\text{SO}_4$ showed an overall water discoloration as high as 82%. It is worth noting that HClO_4 consistently produced lower overall discoloration than Na_2SO_4 under the same experimental conditions. These results could be due to halide electrolytes generating active halide species, which has been suggested in other studies [38]. In their report, Ambauen et al. [38] found that once hydroxyl radicals are formed, secondary reactions may occur when electrochemically active electrolytes are present, including the scavenging of the reactive oxygen species and the secondary production of other less reactive species that are capable of reacting with the organic pollutants under some conditions, resulting in partial chemical oxidation. However, based on the mechanisms for active chloride-mediated electrochemical oxidation, this type of side reaction is not favored because, in most cases, chlorinated byproducts possess a higher toxicity.

On the other hand, using Na_2SO_4 in the EOx-based discoloration of dye water has interesting potential. Previously, we used a BDD anode to remove different industrial sulfonated dye products from water [39]. In that study, we found BBR discoloration ranging from 25% to 95%, which was possibly related to the production of a low and steady concentration of oxygen radical on the BDD surface attacking the dye molecules. The best results were achieved using the highest current density value tested (e.g., 18 mA cm^{-2}), a pH of 3, a 0.5 L laboratory stirred tank reactor, and a 25 cm^2 BDD electrode. In this study, we achieved up to 82% of BBR discoloration for the same reaction time reported previously, but using a BDD electrode area one order of magnitude lower (e.g., 2.5 cm^2).

From this study, pseudo-first-order kinetics were calculated as described above. In the case of HClO_4 medium, the following results were obtained: (\blacktriangle) 0.0038 , (\blacktriangle) 0.0045 , (\blacktriangle) 0.0086 min^{-1} , respectively. For the Na_2SO_4 supporting electrolyte, the following values were obtained: (\blacklozenge) 0.0043 , (\blacklozenge) 0.0161 , (\blacklozenge) 0.0293 min^{-1} , respectively. For all the experimental fittings using the pseudo-first order kinetics model, the minimum R^2 value obtained was 0.99, suggesting that this kinetics model describes the chemical process fairly good. As shown, the k -values found for Na_2SO_4 were about 3.5 times higher than those observed when HClO_4 was used as the supporting electrolyte.

3.2.2. BBR Dye Degradation at Different Current Densities in 0.1 M HClO₄ and FeSO₄

Figure 6a shows water discoloration as a function of FeSO₄ concentration using a current density of 7 mA cm⁻². Slow discoloration was observed for the EOx process alone (◆), and 31% BBR degradation and k -value 0.0030 min⁻¹ were achieved. By adding 1 mM of FeSO₄ to the system (▲), a 38% discoloration and k -value 0.0035 min⁻¹ were achieved. Further increasing the FeSO₄ concentration (e.g., 6 mM (■), and 12 mM (●)) led to water discoloration values of 41% and 46%, respectively, and reaction rate constant values of 0.0038 min⁻¹ and 0.0042 min⁻¹, respectively, were obtained after two hours of treatment [40,41].

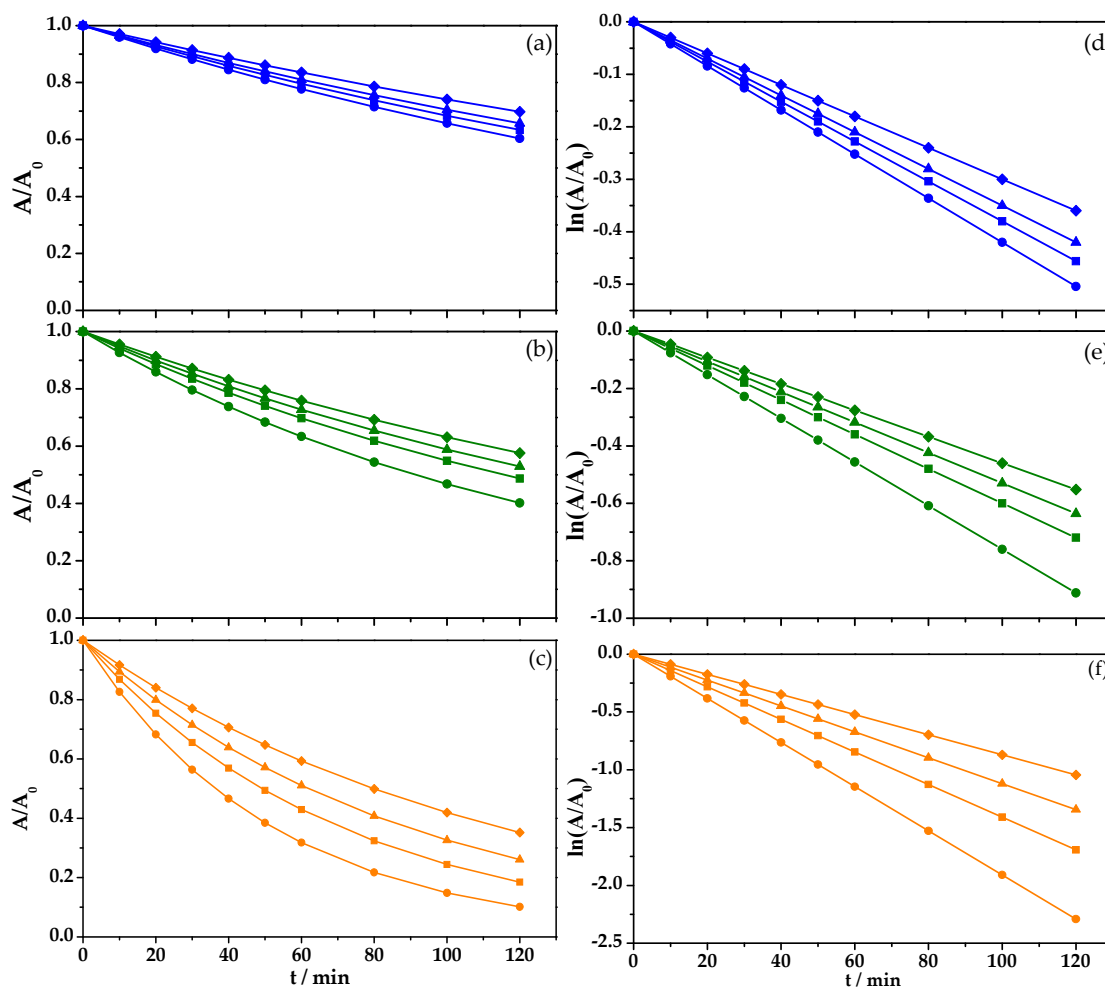


Figure 6. Removal of an aqueous solution of BBR azo dye, $C_0 = 50$ mg/L, during the oxidation process in 0.1 M of HClO₄ with a solution volume of 0.1 L, (a) $j = 7$ mA cm⁻², (b) $j = 15$ mA cm⁻², (c) $j = 30$ mA cm⁻², and fit to first order reaction kinetics (d), (e) y (f), respectively; (◆) BDD without FeSO₄, (▲) 1 mM of FeSO₄, (■) 6 mM of FeSO₄, and (●) 12 mM of FeSO₄.

When current density was increased to 15 mA cm⁻² (Figure 6b), an improvement in discoloration tendency was observed, and the increase in FeSO₄ concentration produced a higher removal speed and discoloration percentage. For the EOx process alone (◆), a 46% discoloration and k_1 -value of 0.0046 min⁻¹ were observed. When 1 mM of FeSO₄ (▲) was used, a 50% discoloration and k_1 -value of 0.0053 min⁻¹ were achieved. Using 6 mM of FeSO₄ (■) produced a 54% discoloration and k_1 -value of 0.0060 min⁻¹. Finally, the process with the greatest discoloration used 12 mM of FeSO₄ (●), generating a 63% discoloration after two hours of treatment and a k_1 -value of 0.0076 min⁻¹.

Further increasing the current density to 30 mA cm⁻² showed the best results, as shown in Figure 6c. Compared with the other conditions tested, the highest discoloration was achieved by

adding 12 mM of FeSO_4 (●) into the solution, followed by adding 6 mM of FeSO_4 (■), 1 mM of FeSO_4 (▲), and finally using the EOX process alone (◆), which produced water discoloration values as high as 93%, 85%, 77%, and 67%, respectively, and k_1 -values of 0.0191 min^{-1} , 0.0141 min^{-1} , 0.0112 min^{-1} , and 0.0087 min^{-1} , respectively.

3.2.3. BBR Dye Degradation at Different Current Densities in 0.05 M of Na_2SO_4 and FeSO_4

Figure 7a shows the degradation of BBR dye (50 mg L^{-1}) using 0.05 M Na_2SO_4 at pH 3 as the support electrolyte after 60 min. It is worth noting that continuous dye degradation was observed for the four different conditions tested: EOX alone and adding 1 mM, 6 mM, and 12 mM of FeSO_4 while operating at a constant current density (7 mA cm^{-2}). The EOX process alone (◆) showed 36% discoloration ($k_1 = 0.0036 \text{ min}^{-1}$). When 1 mM of FeSO_4 (▲) was added, 91% discoloration was achieved ($k_1 = 0.0052 \text{ min}^{-1}$).

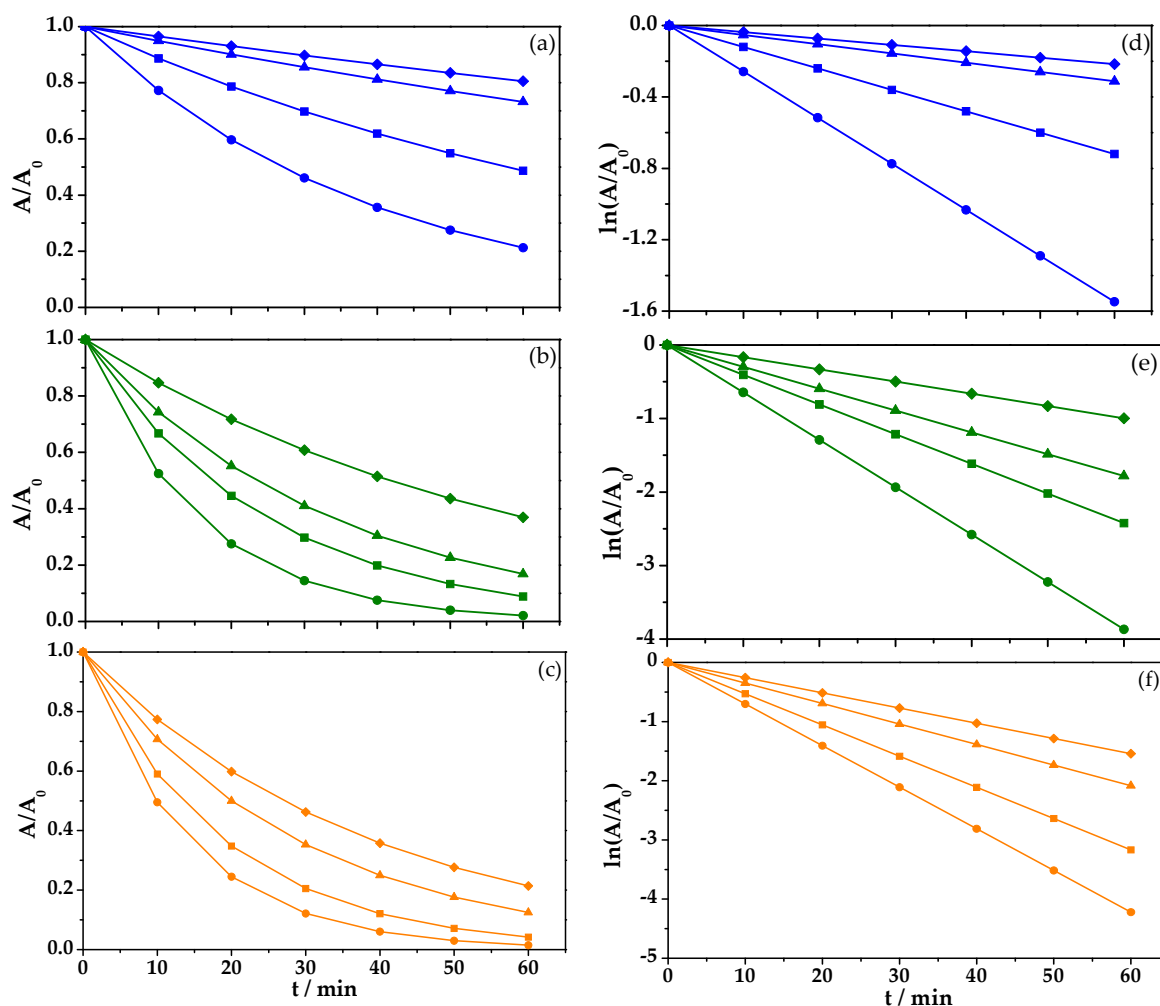


Figure 7. Removal of an aqueous solution of BBR azo dye, $C_0 = 50 \text{ mg/L}$, during the oxidation process in 0.05 M of Na_2SO_4 and at a pH of 3 with a solution volume of 0.1 L, (a) $j = 7 \text{ mA cm}^{-2}$, (b) $j = 15 \text{ mA cm}^{-2}$, (c) $j = 30 \text{ mA cm}^{-2}$, and fit to first order reaction kinetics (d), (e) y (f), respectively; (◆) BDD without FeSO_4 , (▲) 1 mM of FeSO_4 , (■) 6 mM of FeSO_4 , and (●) 12 mM of FeSO_4 .

Water discoloration as high as 94% was observed when 6 mM of FeSO_4 was added (■) ($k_1 = 0.0120 \text{ min}^{-1}$), and finally the faster discoloration (e.g., 96%, $k_1 = 0.0258 \text{ min}^{-1}$) was achieved after 60 min of treatment using 12 mM of FeSO_4 (●).

Increasing the current density to 15 mA cm^{-2} (Figure 7b) generated better results for BBR dye discoloration for shorter process times. When EOX was used alone (◆), 63% ($k_1 = 0.0166 \text{ min}^{-1}$) was

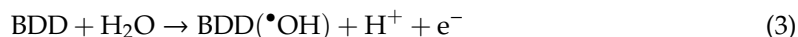
observed. When 1 mM of FeSO_4 (\blacktriangle) was added, 80% dye removal ($k_1 = 0.0297 \text{ min}^{-1}$) was achieved after 60 min. By increasing FeSO_4 to 6 mM (\blacksquare), 89% ($k_1 = 0.0404 \text{ min}^{-1}$) was reached and, when using 12 mM of FeSO_4 (\bullet), 96% ($k_1 = 0.0645 \text{ min}^{-1}$) was reached after 60 min.

The same tendency was observed when the highest current density (30 mA cm^{-2}) was applied, as shown in Figure 7c. In this case, using 12 mM of FeSO_4 (\bullet) generated 98% discoloration ($k_1 = 0.0703 \text{ min}^{-1}$), and using 6 mM of FeSO_4 (\blacksquare) generated 95% discoloration ($k_1 = 0.0528 \text{ min}^{-1}$). Using 1 mM of FeSO_4 (\blacktriangle), 87% discoloration ($k_1 = 0.0347 \text{ min}^{-1}$) was achieved, and finally EOx alone (\blacklozenge) only reached 78% discoloration ($k_1 = 0.0257 \text{ min}^{-1}$) after 60 min.

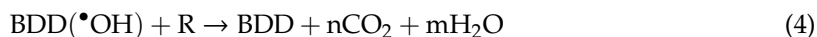
Based on these results, a combined BBR oxidation process is proposed. For the first case where we used FeSO_4 and HClO_4 as an electrolyte, the oxidation process would occur directly on the BDD electrode (EOx) and indirectly (chemically) through the hydroxyl radicals (resulting from water oxidation) and ferrate ions (resulting from FeSO_4 oxidation), as in Scheme 1, reactions 4, 5 and 8. For the second case, where FeSO_4 and Na_2SO_4 were used as electrolyte, the BBR oxidation process occurs directly on the BDD electrode (EOx, reaction 5) and indirectly (chemically) through the hydroxyl radicals (resulting from water oxidation, reactions 3 and 4), ferrate (VI) ions (resulting from FeSO_4 oxidation, reactions 7 and 8) and persulfates (resulting from the oxidation of Na_2SO_4 , reactions 9 and 10), as in the Scheme 2 [42]. The formation of persulfate causes the latter case to be more effective in the oxidation of the BBR.

Based on the above, the simultaneous processes of EOx and the generation of ferrate ions in situ can be summarized with the following reactions [21]:

1. Discharge of water into the system and generation of oxygen radicals ($\bullet\text{OH}$).



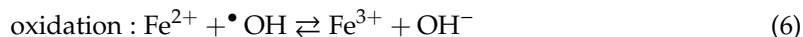
2. Oxidation of contaminants by oxygen radicals ($\bullet\text{OH}$).



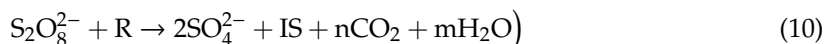
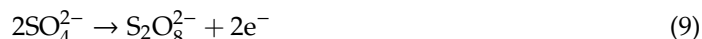
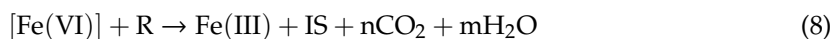
3. Oxidation of contaminants on BDD.



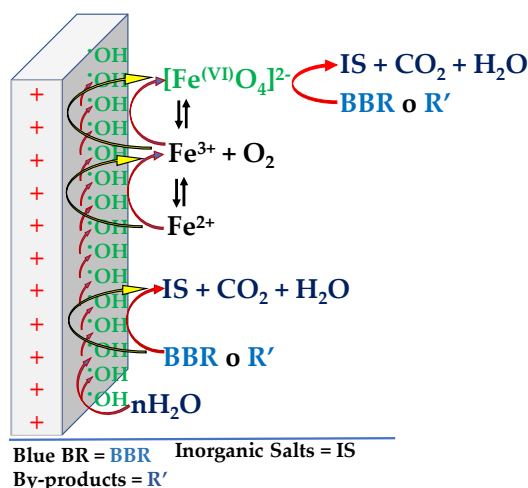
4. Generation of [Fe(VI)] from FeSO_4 on BDD.



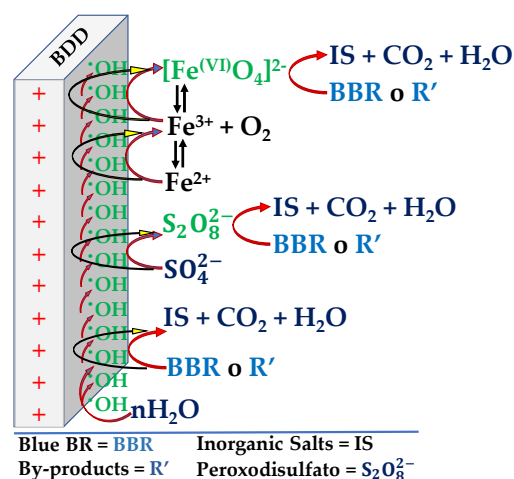
5. Oxidation of organic compounds by [Fe(VI)] and $\text{S}_2\text{O}_8^{2-}$:



For this study, stages (e) and (f) were avoided by working at low FeSO_4 concentrations, which promoted a synergistic effect in stages (b) and (d).



Scheme 1. Representation of the reactions involved on BDD substrate electrode held in FeSO_4 and 0.1 M of HClO_4 .



Scheme 2. Representation of the reactions involved on BDD substrate electrode held in FeSO_4 and 0.05 M Na_2SO_4 .

3.2.4. COD Determinations and Byproduct Evolution

In Figure 8, COD reduction is shown by comparing EOX alone (♦) with the in situ generation of $[\text{Fe}(\text{VI})]$ (●). Electro-oxidation alone was able to achieve 37% COD removal after 90 min of treatment. In the case of ferrate generation, 61% COD removal was obtained, suggesting electrogenerated $[\text{Fe}(\text{VI})]$ ions directly influence a decrease in COD by carrying out pollutant degradation more efficiently and reducing the amount of oxidable matter in the solution [43,44].

Figure 8a shows the accumulation of a low amount of carboxylic acids generated during the EOX process alone (♦) and while testing the simultaneous EOX/ $[\text{Fe}(\text{VI})]$ processes using 12 mM of Fe_2O_4 (●) at 30 mA cm^{-2} . The carboxylic acid quantified from BBR degradation was oxalic acid. Figure 8b shows that oxalic acid generation contributed only almost 20 mg/L using the EOX process alone, whereas adding 12 mM of FeSO_4 produced only 2 mg L^{-1} under the simultaneous EOX/ $[\text{Fe}(\text{VI})]$ process. These results suggest that the degradative pathway of BBR produces carboxylic acid because of the combined action of $\cdot\text{OH}$ and ferrate ions generated in the solution [45–49].

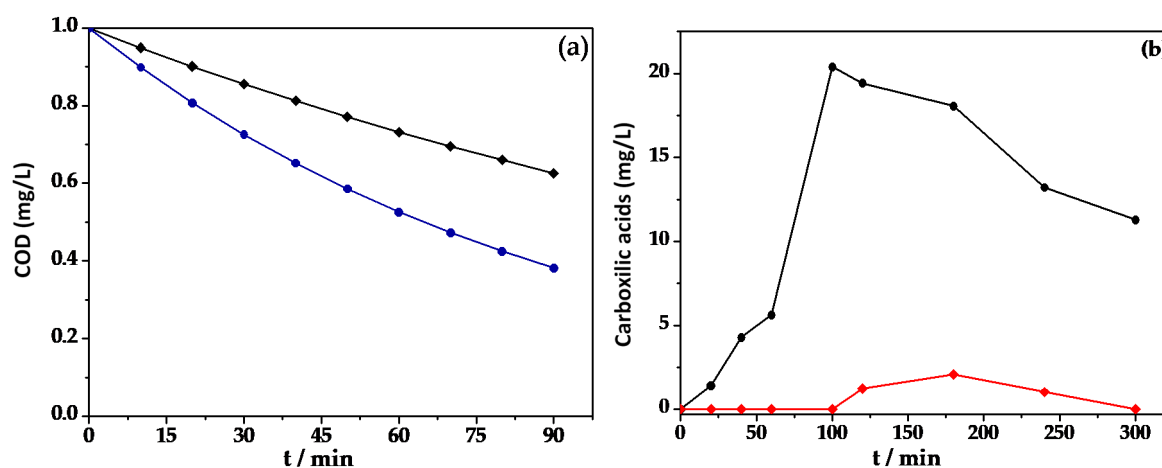


Figure 8. (a) Variation of COD abatement for 50 mg/L of BBR azo dye using BDD electrolysis without FeSO_4 (◆) and the simultaneous EOx/[Fe(VI)] process using 12 mM of FeSO_4 (●) in 0.05 M of Na_2SO_4 at a pH of 3 at 30 mA cm^{-2} . (b) Evolution of the concentration of oxalic acid produced during the degradation of 0.4 L of 50 mg/L BBR solution in 0.05 M of Na_2SO_4 at a pH of 3 and 35°C using BDD without FeSO_4 (●) and the simultaneous EOx/[Fe(VI)] process using 12 mM of FeSO_4 (◆) at 30 mA cm^{-2} .

4. Conclusions

Electrochemical characterization using cyclic voltammetry confirms the in situ electrogeneration of ferrate ions on the BDD surface by adding FeSO_4 in both the sulfate and perchloric acid media. The use of HClO_4 produced discoloration efficiency close to 93% after 120 min of treatment when 12 mM of FeSO_4 was added. However, faster degradation rates were observed using the sulfate medium, which achieved up to 98% of color reduction in 60 min of treatment when 12 mM of FeSO_4 was added and a current density of 30 mA cm^{-2} was applied. A COD abatement as high as 63% was observed when the highest FeSO_4 concentration was added to the reaction mixture using the highest current density value. The byproduct analysis detected the presence of only one carboxylic acid (oxalic acid), which was rapidly oxidized by the simultaneous EOx/[Fe(VI)] process. These were identified as the best treatment conditions because they allowed some smaller amount reaction byproducts to accumulate.

Based on the obtained results, it was possible to demonstrate the viability of the simultaneous generation of both oxidant species, the free radical and the ferrate ion, which opens up an important opportunity to carry out not only the degradation of dyes, but also other organic compounds that are difficult to remove. This work provides an advance in the study of the simultaneous generation of oxidant species to the scientific community interested in this subject. In the future, the challenge will be understanding the reaction mechanisms.

Author Contributions: Conceptualization, P.J.E.-M. and J.M.P.-H.; methodology, P.J.E.-M. and J.M.P.-H.; validation, M.C.; formal analysis, M.C., P.J.E.-M. and J.M.P.-H.; resources, M.C. and P.J.E.-M.; writing—original draft preparation, M.C. and P.J.E.-M.; writing—review and editing, P.J.E.-M. and J.M.P.-H.; visualization, supervision, J.M.P.-H.; project administration, J.M.P.-H.; funding acquisition J.M.P.-H., O.R., A.P., E.R.B. and S.G.-G. All authors have read and agreed to the published version of the manuscript.

Funding: The authors would like to acknowledge the economic support of the Universidad de Guanajuato.

Acknowledgments: O.M. Rodríguez-Narvaez and Alain Picos would like to thank CONACYT for a graduate fellowship. The authors are also grateful to Nicole Damon (DRI) for her editorial review.

Conflicts of Interest: The authors declare no conflict of interest.

References

- Alcocer, S.; Picos, A.; Uribe, A.R.; Pérez, T.; Peralta-Hernández, J.M. Comparative study for degradation of industrial dyes by electrochemical advanced oxidation processes with BDD anode in a laboratory stirred tank reactor. *Chemosphere* **2018**, *205*, 682–689. [[CrossRef](#)]

2. Alsheyab, M.; Jiang, J.-Q.; Stanford, C. On-line production of ferrate with an electrochemical method and its potential application for wastewater treatment—A review. *J. Environ. Manag.* **2009**, *90*, 1350–1356. [[CrossRef](#)]
3. Ambauen, N.; Muff, J.; Mai, N.L.; Hallé, C.; Trinh, T.T.; Meyn, T. Insights into the kinetics of intermediate formation during electrochemical oxidation of the organic model pollutant salicylic acid in chloride electrolyte. *Water* **2019**, *11*, 1322. [[CrossRef](#)]
4. Bennett, J.A.; Wang, J.; Show, Y.; Swain, G.M. Effect of sp²-Bonded Nondiamond Carbon Impurity on the Response of Boron-Doped Polycrystalline Diamond Thin-Film Electrodes. *J. Electrochem. Soc.* **2004**, *151*, E306. [[CrossRef](#)]
5. Cataldo-Hernández, M.A.; Govindarajan, R.; Bonakdarpour, A.; Mohseni, M.; Wilkinson, D.P. Electrosynthesis of ferrate in a batch reactor at neutral conditions for drinking water applications. *Can. J. Chem. Eng.* **2018**, *96*, 1648–1655. [[CrossRef](#)]
6. Cataldo-Hernández, M.; Stewart, M.; Bonakdarpour, A.; Mohseni, M.; Wilkinson, D.P. Degradation of ferrate species produced electrochemically for use in drinking water treatment applications. *Can. J. Chem. Eng.* **2018**, *96*, 1045–1052. [[CrossRef](#)]
7. Cerreta, G.; Roccamante, M.A.; Oller, I.; Malato, S.; Rizzo, L. Contaminants of emerging concern removal from real wastewater by UV/free chlorine process: A comparison with solar/free chlorine and UV/H₂O₂ at pilot scale. *Chemosphere* **2019**, *236*, 124354. [[CrossRef](#)] [[PubMed](#)]
8. Cho, M.; Lee, Y.; Choi, W.; Chung, H.; Yoon, J. Study on Fe (VI) species as a disinfectant: Quantitative evaluation and modeling for inactivating *Escherichia coli*. *Water Res.* **2006**, *40*, 3580–3586. [[CrossRef](#)]
9. Coria, G.; Pérez, T.; Sirés, I.; Brillas, E.; Nava, J.L. Abatement of the antibiotic levofloxacin in a solar photoelectro-Fenton flow plant: Modeling the dissolved organic carbon concentration-time relationship. *Chemosphere* **2018**, *198*, 174–181. [[CrossRef](#)]
10. Dávila, O.O.; Bergeron, L.L.; Gutiérrez, P.R.; Jiménez, M.M.D.; Sirés, I.; Brillas, E.; Roig Navarro, A.F.; Arandes, J.B.; Llopis, J.V.S. Electrochemical oxidation of dibenzothiophene compounds on BDD electrode in acetonitrile–water medium. *J. Electroanal. Chem.* **2019**, *847*, 113172. [[CrossRef](#)]
11. Deng, Y.; Jung, C.; Liang, Y.; Goodey, N.; Waite, T.D. Ferrate (VI) decomposition in water in the absence and presence of natural organic matter (NOM). *Chem. Eng. J.* **2018**, *334*, 2335–2342. [[CrossRef](#)]
12. Denvir, A.; Pletcher, D. Electrochemical generation of ferrate Part I: Dissolution of an iron wool bed anode. *J. Appl. Electrochem.* **1996**, *26*, 815–822. [[CrossRef](#)]
13. Diaz, M.; Cataldo, M.; Ledezma, P.; Keller, J.; Doederer, K. Unravelling the mechanisms controlling the electro-generation of ferrate using four iron salts in boron-doped diamond electrodes. *J. Electroanal. Chem.* **2019**, *854*, 113501. [[CrossRef](#)]
14. Dos Santos, A.B.; Cervantes, F.J.; van Lier, J.B. Review paper on current technologies for decolourisation of textile wastewaters: Perspectives for anaerobic biotechnology. *Bioresour. Technol.* **2007**, *98*, 2369–2385. [[CrossRef](#)] [[PubMed](#)]
15. Elgrishi, N.; Rountree, K.J.; McCarthy, B.D.; Rountree, E.S.; Eisenhart, T.T.; Dempsey, J.L. A Practical Beginner's Guide to Cyclic Voltammetry. *J. Chem. Educ.* **2018**, *95*, 197–206. [[CrossRef](#)]
16. Eng, Y.Y.; Sharma, V.K.; Ray, A.K. Ferrate(VI): Green chemistry oxidant for degradation of cationic surfactant. *Chemosphere* **2006**, *63*, 1785–1790. [[CrossRef](#)]
17. Espinoza-Montero, P.J.; Vasquez-Medrano, R.; Ibanez, J.G.; Frontana-Urbe, B.A. Efficient anodic degradation of phenol paired to improved cathodic production of H₂O₂ at BDD electrodes. *J. Electrochem. Soc.* **2013**, *160*, G3171–G3177. [[CrossRef](#)]
18. Espinoza, C.; Romero, J.; Villegas, L.; Cornejo-Ponce, L.; Salazar, R. Mineralization of the textile dye acid yellow 42 by solar photoelectro-Fenton in a lab-pilot plant. *J. Hazard. Mater.* **2016**, *319*, 24–33. [[CrossRef](#)]
19. Wood, R.H. The Heat, Free Energy and Entropy of the Ferrate(VI) Ion. *J. Am. Chem. Soc.* **2002**, *80*, 2038–2041. [[CrossRef](#)]
20. Ibanez, J.G.; Tellez-Giron, M.; Alvarez, D.; Garcia-Pintor, E. Laboratory Experiments on the Electrochemical Remediation of the Environment. Part 6: Microscale Production of Ferrate. *J. Chem. Educ.* **2004**, *81*, 251. [[CrossRef](#)]
21. Jiang, J.-Q.; Lloyd, B. Progress in the development and use of ferrate(VI) salt as an oxidant and coagulant for water and wastewater treatment. *Water Res.* **2002**, *36*, 1397–1408. [[CrossRef](#)]
22. Jiang, J.Q. Advances in the development and application of ferrate(VI) for water and wastewater treatment. *J. Chem. Technol. Biotechnol.* **2014**, *89*, 165–177. [[CrossRef](#)]

23. Kanari, N.; Ostrosi, E.; Diliberto, C.; Filippova, I.; Shallari, S.; Allain, E.; Diot, F.; Patisson, F.; Yvon, J. Green Process for Industrial Waste Transformation into Super-Oxidizing Materials Named Alkali Metal Ferrates (VI). *Materials* **2019**, *12*, 1977. [[CrossRef](#)] [[PubMed](#)]
24. Lee, J.; Tryk, D.A.; Fujishima, A.; Park, S.-M. Electrochemical generation of ferrate in acidic media at boron-doped diamond electrodes. *Chem. Commun.* **2002**, 486–487. [[CrossRef](#)]
25. Lescuras-Darrou, V.; Lapicque, F.; Valentin, G. Electrochemical ferrate generation for waste water treatment using cast irons with high silicon contents. *J. Appl. Electrochem.* **2002**, *32*, 57–63. [[CrossRef](#)]
26. Liu, J.; Zhang, Z.; Liu, Z.; Zhang, X. Integration of ferrate (VI) pretreatment and ceramic membrane reactor for membrane fouling mitigation in reclaimed water treatment. *J. Membr. Sci.* **2018**, *552*, 315–325. [[CrossRef](#)]
27. Mácová, Z.; Bouzek, K.; Híveš, J.; Sharma, V.K.; Terry, R.J.; Baum, J.C. Research progress in the electrochemical synthesis of ferrate(VI). *Electrochim. Acta* **2009**, *54*, 2673–2683. [[CrossRef](#)]
28. Martínez-huitle, C.A.; Brillas, E. Electrochemical Alternatives for Drinking Water Disinfection. *Angew. Int. Ed. Chem.* **2008**, *47*, 1998–2005. [[CrossRef](#)]
29. Morales, U.; Escudero, C.J.; Rivero, M.J.; Ortiz, I.; Rocha, J.M.; Peralta-Hernández, J.M. Coupling of the electrochemical oxidation (EO-BDD)/photocatalysis (TiO₂-Fe-N) processes for degradation of acid blue BR dye. *J. Electroanal. Chem.* **2018**, *808*, 180–188. [[CrossRef](#)]
30. Oriol, R.; del Pilar Bernícola, M.; Brillas, E.; Cabot, P.L.; Sirés, I. Paired electro-oxidation of insecticide imidacloprid and electrodenitrification in simulated and real water matrices. *Electrochim. Acta* **2019**, *317*, 753–765. [[CrossRef](#)]
31. Pacheco-Álvarez, M.O.A.; Picos, A.; Pérez-Segura, T.; Peralta-Hernández, J.M. Proposal for highly efficient electrochemical discoloration and degradation of azo dyes with parallel arrangement electrodes. *J. Electroanal. Chem.* **2019**, *838*, 195–203. [[CrossRef](#)]
32. Panizza, M.; Cerisola, G. Application of diamond electrodes to electrochemical processes. *Electrochim. Acta* **2005**, *51*, 191–199. [[CrossRef](#)]
33. Villanueva-Rodríguez, M.; Hernández-Ramírez, A.; Peralta-Hernández, J.M.; Bandala, E.R.; Quiroz-Alfaro, M.A. Enhancing the electrochemical oxidation of acid-yellow 36 azo dye using boron-doped diamond electrodes by addition of ferrous ion. *J. Hazard. Mater.* **2009**, *167*, 1226–1230. [[CrossRef](#)] [[PubMed](#)]
34. Villanueva-Rodríguez, M.; Sánchez-Sánchez, C.M.; Montiel, V.; Brillas, E.; Peralta-Hernández, J.M.; Hernández-Ramírez, A. Characterization of ferrate ion electrogeneration in acidic media by voltammetry and scanning electrochemical microscopy. Assessment of its reactivity on 2, 4-dichlorophenoxyacetic acid degradation. *Electrochim. Acta* **2012**, *64*, 196–204.
35. Queiroz, N.M.P.; Sirés, I.; Zanta, C.L.P.S.; Tonholo, J.; Brillas, E. Removal of the drug procaine from acidic aqueous solutions using a flow reactor with a boron-doped diamond anode. *Sep. Purif. Technol.* **2019**, *216*, 65–73. [[CrossRef](#)]
36. Rice, E.W.; Baird, R.B.; Eaton, A.D.; Clesceri, L.S. *Standard Methods for the Examination of Water and Wastewater*; American Public Health Association: Washington, DC, USA, 2012; p. 541.
37. Ruiz, E.J.; Hernández-Ramírez, A.; Peralta-Hernández, J.M.; Arias, C.; Brillas, E. Application of solar photoelectro-Fenton technology to azo dyes mineralization: Effect of current density, Fe²⁺ and dye concentrations. *Chem. Eng. J.* **2011**, *171*, 385–392. [[CrossRef](#)]
38. Serrano, K.; Michaud, P.A.; Comminellis, C.; Savall, A. Electrochemical preparation of peroxodisulfuric acid using boron doped diamond thin film electrodes. *Electrochim. Acta* **2002**, *48*, 431–436. [[CrossRef](#)]
39. Sharma, V.K. Potassium ferrate(VI): Properties and applications. *ACS Div. Environ. Chem. Prepr.* **2000**, *40*, 131–132.
40. Sharma, V.K.; Burnett, C.R.; O'Connor, D.B. Ferrate(VI) and ferrate(V) oxidation of thiocyanate. *ACS Div. Environ. Chem. Prepr.* **2000**, *40*, 600–601.
41. Sharma, V.K. Potassium ferrate(VI): An environmentally friendly oxidant. *Adv. Environ. Res.* **2002**, *6*, 143–156. [[CrossRef](#)]
42. Sharma, V.K.; Kazama, F.; Jiangyong, H.; Ray, A.K. Ferrates (iron(VI) and iron(V)): Environmentally friendly oxidants and disinfectants. *J. Water Health* **2005**, *3*, 45–58. [[CrossRef](#)] [[PubMed](#)]
43. Sharma, V.K.; Rivera, W.; Joshi, V.N.; Millero, F.J.; O'Connor, D. Ferrate(VI) Oxidation of Thiourea. *Environ. Sci. Technol.* **1999**, *33*, 2645–2650. [[CrossRef](#)]

44. Talaiekhosani, A.; Talaei, M.R.; Rezaia, S. An overview on production and application of ferrate (VI) for chemical oxidation, coagulation and disinfection of water and wastewater. *J. Environ. Chem. Eng.* **2017**, *5*, 1828–1842. [[CrossRef](#)]
45. Thiam, A.; Salazar, R. Fenton-based electrochemical degradation of metolachlor in aqueous solution by means of BDD and Pt electrodes: Influencing factors and reaction pathways. *Environ. Sci. Pollut. Res.* **2019**, *26*, 2580–2591. [[CrossRef](#)]
46. Pérez, T.; Sirés, I.; Brillas, E.; Nava, J.L. Solar photoelectro-Fenton flow plant modeling for the degradation of the antibiotic erythromycin in sulfate medium. *Electrochim. Acta* **2017**, *228*, 45–56. [[CrossRef](#)]
47. Potts, M.E.; Churchwell, D.R. Removal of Radionuclides in Wastewaters Utilizing Potassium ferrate(VI). *Water Environ. Res.* **1994**, *66*, 107–109. [[CrossRef](#)]
48. Ye, Z.; Brillas, E.; Centellas, F.; Cabot, P.L.; Sirés, I. Electro-Fenton process at mild pH using Fe(III)-EDDS as soluble catalyst and carbon felt as cathode. *Appl. Catal. B Environ.* **2019**, *257*, 117907. [[CrossRef](#)]
49. Lee, Y.; Cho, M.K.; Kim, J.Y.; Yoon, J. Chemistry of Ferrate (Fe(VI)) in Aqueous Solution and its Applications as a Green Chemical. *J. Ind. Eng. Chem.* **2004**, *10*, 161–171.



© 2020 by the authors. Licensee MDPI, Basel, Switzerland. This article is an open access article distributed under the terms and conditions of the Creative Commons Attribution (CC BY) license (<http://creativecommons.org/licenses/by/4.0/>).